

Brain Tumor Segmentation in Magnetic Resonance Images using Genetic Algorithm Clustering and AdaBoost Classifier

Gustavo C. Oliveira¹, Renato Varoto² and Alberto Cliquet Jr.^{1,2,3}

¹University of São Paulo Interunits Graduate Program in Bioengineering, University of São Paulo, São Carlos - SP, Brazil

²Department of Orthopedics and Traumatology, University of Campinas (UNICAMP), Campinas - SP, Brazil

³Department of Electrical and Computer Engineering, University of São Paulo, São Carlos - SP, Brazil

Keywords: Image Segmentation, Glioma, Genetic Algorithm, AdaBoost Classifier.

Abstract: We present a technique for automatic brain tumor segmentation in magnetic resonance images, combining a modified version of a Genetic Algorithm Clustering method with an AdaBoost Classifier. In a group of 42 FLAIR images, segmentations produced by the algorithm were compared to the ground truth information produced by radiologists. The mean Dice similarity coefficient reached by the algorithm was 70.3%. In most cases, the AdaBoost classifier increased the quality of the segmentation, improving, on average, the DSC in about 10%. Our implementation of the Genetic Algorithm Clustering method presents improvements compared to the original method. The use of a fixed, small number of groups and smaller population allowed for less computational effort. In addition, adaptive restriction in the initial segmentation was achieved by using the information of the groups with highest and 2nd-highest mean intensities. By exploring intensity and spatial information of the pixels, the AdaBoost classifier improved segmentation results.

1 INTRODUCTION

Glioma is a type of brain tumor that originates in the glial cells, which support and surround neurons in the brain. Growing within the tissue of the brain and often mixing with healthy areas, it's the most frequent primary brain tumor in adults, representing 33% of all cases. By pressing on the spinal cord or the brain, gliomas can cause many symptoms, such as seizures, personality changes, weakness in the face or limbs, problems with speech, vision loss and dizziness. In its less aggressive form, known as low-grade gliomas, patients have a life expectancy of several years, and in its more aggressive form, known as high-grade gliomas, patients have a median survival rate of two years or less. The most common treatment for gliomas is surgery, which may be followed by radiation therapy and chemotherapy (Menze et al., 2015; Johns Hopkins Medicine Health Library, 2017).

Diagnosis of glioma tumors involves an analysis of the patient's medical history, neurological exams and scans of the brain – magnetic resonance imaging and computed tomography. Throughout the treatment process, imaging protocols are used to follow disease progression and evaluate the success of the chosen strategy. Analysis of those images usually relies on

rudimentary quantitative measures or qualitative criteria – such as the largest diameter visible from axial images of the lesion or presence of characteristic hyper-intense tissue (Menze et al., 2015; Johns Hopkins Medicine Health Library, 2017).

In this context, the development of computer aided-diagnosis (CAD) systems that can automatically analyze brain tumor scans and replace the current evaluation methods with more reproducible and accurate measurements could significantly improve the diagnosis, treatment and follow-up processes by providing standardized criteria for tumor characterization and time efficiency (Menze et al., 2015; Emblem et al., 2009). More specifically, CADs could perform the segmentation task, separating the different tumor tissues from healthy brain tissue, to extract the patient specific clinical information, along with their diagnostic features. In the last years, a great variety of segmentation methods was proposed, combining threshold-based, model-based, region-based and pixel classification techniques (Gordillo et al., 2013). Comparing these methods, however, is problematic, since they are usually validated with different performance metrics, on small and private datasets and using different imaging modalities (Menze et al., 2015).

To overcome these difficulties, the Multimodal

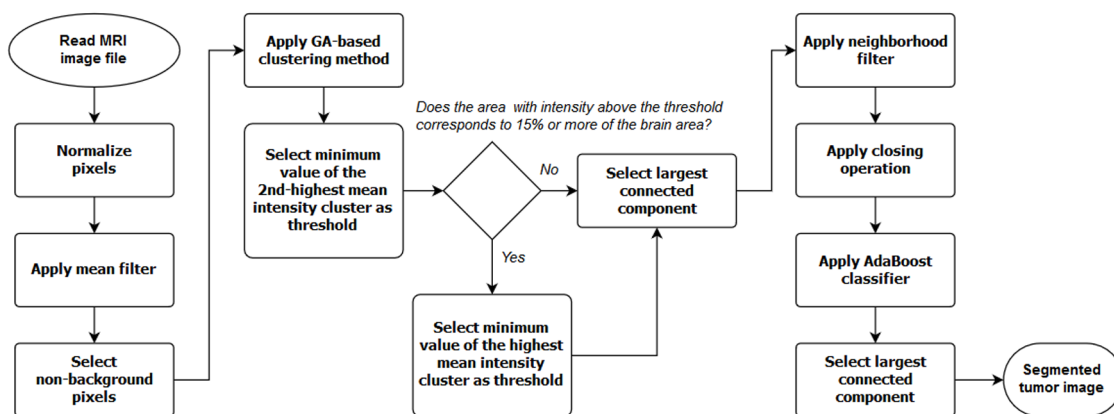


Figure 1: Flowchart of the algorithm.

Brain Tumor Image Segmentation (BRATS) challenge was organized. In this challenge, 20 state-of-art algorithms were applied to the same dataset and evaluated in three different tasks: segmentation of the “whole” tumor (including edema, non-enhancing solid core, active core and non-solid core), segmentation of the tumor “core” (including all classes except edema), and segmentation of the “active tumor” (containing only the “active core”). It was found that no single method ranked in the top five for all tasks - different algorithms performed best for different sub-regions. The development of algorithms for brain tumor segmentation continues to attract interest of the research community (Menze et al., 2015).

Kole and Halder proposed an automatic method for brain tumor detection and isolation of tumor cells from magnetic resonance images (MRI) using a genetic algorithm-based clustering method (Kole and Halder, 2012). In this paper, an extension of their technique is presented, combining their clustering method with morphological operation, filters and an AdaBoost classifier.

2 MATERIALS AND METHODS

2.1 Algorithm

The flowchart presented in Figure 1 gives an overview of the proposed technique, which operates as follows. First, pixels in the image are normalized and a 3x3x3 mean filter is applied. Non-background pixels are then selected and grouped into clusters according to their intensity values using the genetic algorithm (GA)-based clustering method (Kole and Halder, 2012).

Let K represent the number of clusters that the pixels of the image will be divided into. K ranges

from 2 to 5 - i.e. pixels will be divided into 2, 3, 4 and 5 clusters. In the GA-based clustering method, each chromosome of the population consists of K numbers, intensity values which represent the centers of each cluster. At each generation, a fitness function is computed in order to find and select the center values that best divide the pixels into K clusters by minimizing intra-cluster spread. The next generation is then created using mutation and cross-over processes. This is repeated through several iterations. Then K is increased, new chromosomes are generated and the evolutionary process is repeated. This continues until K reaches its final value. Finally, pixels are grouped using the most appropriate number of clusters, which is the one that minimizes the validity index (Kole and Halder, 2012). Overall, the method can be summarized in the following steps:

1. For each number of groups K , repeat steps 2 to 7.
2. Generate initial values of each chromosome of the population.
3. Calculate the fitness value of each chromosome.
4. Preserve the chromosome with highest fitness value found so far.
5. Select chromosomes using the Roulette Wheel algorithm.
6. Create chromosomes of the next generation through mutation and cross-over.
7. Until termination condition is reached, repeat steps 3 to 6.
8. Compute the clustering validity index for the fittest chromosome of all values of K .
9. Cluster pixels using the value of K that minimizes the validity index.

For more details, please refer to the original article (Kole and Halder, 2012).

After finding the clusters, thresholding is performed to obtain a binary image. Selection of the threshold value is based on the clusters: the first choice is to use the minimum value of the cluster with 2nd highest mean intensity. Pixels with intensity value above the threshold are marked as tumor (i.e. they're assigned the value "1"), whereas pixels with intensity value below the threshold are marked as background (i.e. they're assigned the value "0"). If the thresholding operation results in a segmentation that selects more than 15% of the area of the brain as tumor, then the first binary image is abandoned and the minimum value of the cluster with highest mean intensity is chosen as the threshold value. The threshold operation is repeated, producing a new binary image.

Once the binary image is produced, the program selects the largest connected component and applies to it a neighborhood filter. This filter computes, for each pixel, the number of tumor pixels that are 8-connected to it, i.e. the number of tumor pixels that touches one of the edges or corners of the pixel. If this number is 4 or more, then the current pixel is included. If it's 2 or less, the current pixel is excluded or not included in the tumor area (Gibbs et al., 1996; Sonka et al., 2014). Following the filtering step, holes in the segmented area are removed by applying the morphological closing operation iteratively, using a small disk as the structuring element.

Finally, an AdaBoost classifier is used to improve the segmentation. The AdaBoost algorithm is a technique used to create a strong, accurate classifier by combining weak classifiers, assumed to be better than random guessing in correctly classifying the data. For a training set of multidimensional data points, a classifier will assign to each data point a label, either +1 or -1. An exponential error function is used to rank all the weak classifiers based on the number of correct and incorrect classifications. AdaBoost proceeds by systematically extracting one classifier of the pool in each of the iterations, by focusing on the ones that can help with the misclassified data points. After extracting a weak classifier, AdaBoost assigns a weight to it. The stronger classifier is then given by the group of extracted weak classifiers combined with their assigned weights (Freund and Schapire, 1995; Schapire, 1999; Alpaydin, 2014).

In our method, the AdaBoost algorithm classifies pixels according to three features: intensity value and coordinates "x" and "y", which determine the pixel position in the slice. Preliminary class information, used as training data, is given by the binary image produced by the previous steps.

The AdaBoost classifier is applied one slice at a

time, from bottom to top. At each slice, the mean pixel intensity and standard deviation for healthy tissue and for tumor tissue are calculated. Non-background pixels are selected, and data features for each pixel are extracted. Since AdaBoost seems especially sensible to noise (Schapire, 1999; Alpaydin, 2014), pixels that present intensity values that are more than one standard deviation either above or below the mean are considered outliers and are excluded. The selected pixels are then used to train the classifier, building a model that will be used to classify pixels in the slice immediately above. This process continues until there are no more slices to be classified. The largest connected component is then selected, representing the final result of the segmentation process.

In summary, our method uses as basis for an initial segmentation the GA-based clustering method (Kole and Halder, 2012). Then, it refines the segmentation by applying the neighborhood filter, the morphological closing operation and the AdaBoost classifier.

The algorithm was implemented using MATLAB, from The Mathworks, Inc. Tests using MRI images were performed on a Windows 10 PC, 8 GB RAM, Intel(R) Core(TM) i7-5500U CPU @ 2.40 GHz.

2.2 Image Dataset and Evaluation Metric

The proposed method was used to perform "whole" tumor segmentation of low-grade glioma tumors on tridimensional T2-weighted FLAIR images. These images, as well as the ground truth information, were extracted from the 2015 Multimodal Brain Tumor Image Segmentation Benchmark (BRATS) challenge database, which is the largest public dataset of its type, containing a great variety of cases. All of them were preprocessed in order to homogenize the data and remove the skulls, guaranteeing anonymization of the patients (Menze et al., 2015). Two images from the original database were excluded since the assumption that the largest component represents the tumor did not hold for them, resulting in a total of 42 test cases.

Ground truth information was constructed based on manual annotations performed by a team of trained radiologists (Menze et al., 2015). Segmentation results were compared to the ground truth information using the Dice similarity coefficient (DSC). The DSC is based on the computation of the area of overlap between segmented region and ground truth, and it is considered a very attractive metric because of its simplicity, being widely used for evaluation of segmentation algorithms. It is calculated using the following

Table 1: Test cases and the respective DSC values obtained.

Case	DSC - Close	DSC - Final	Case	DSC - Close	DSC - Final
pat101	0.724426	0.814401	pat325	0.155660	0.697677
pat103	0.372215	0.796679	pat330	0.203043	0.562035
pat109	0.853468	0.811614	pat346	0.447613	0.537141
pat130	0.793343	0.419234	pat351	0.538680	0.743219
pat141	0.857224	0.807989	pat387	0.029067	0.132889
pat152	0.912758	0.735904	pat393	0.461802	0.793748
pat175	0.425288	0.930112	pat402	0.879448	0.880263
pat177	0.095312	0.125464	pat410	0.038867	0.038867
pat202	0.468797	0.473320	pat413	0.586182	0.439421
pat241	0.551048	0.926315	pat420	0.430172	0.716093
pat249	0.732158	0.821051	pat428	0.602043	0.774421
pat254	0.800027	0.931246	pat442	0.141631	0.361035
pat255	0.551579	0.860707	pat449	0.863212	0.831586
pat261	0.704085	0.780075	pat451	0.718508	0.693981
pat266	0.688977	0.791121	pat462	0.590710	0.908526
pat276	0.742505	0.576310	pat466	0.938959	0.950347
pat282	0.668736	0.801328	pat470	0.796363	0.832161
pat298	0.898178	0.769875	pat480	0.495931	0.863931
pat299	0.845593	0.832962	pat483	0.841977	0.912231
pat307	0.458549	0.695856	pat490	0.601234	0.710943
pat312	0.613672	0.703324	pat493	0.856309	0.747976
Average Close DSC	0.594651		Average Final DSC	0.703175	

equation:

$$DSC = \frac{2 \times |T_1 \cap P_1|}{|T_1| + |P_1|} \quad (1)$$

where $T \in \{0, 1\}$ and $P \in \{0, 1\}$ are binary maps representing the ground truth and the algorithm's segmentation, respectively; T_1 and P_1 represent the pixels where $T = 1$ and $P = 1$, respectively; \cap is the logical AND operator and $|T_1|$ and $|P_1|$ represent the size of the sets T_1 and P_1 - the number of pixels belonging to them (Sonka et al., 2014; Menze et al., 2015).

3 RESULTS

Table 1 presents the DSC values obtained for each test case by comparing the segmentations produced by the algorithm to the ground truth information. The "DSC - Close" columns present the DSC values for the segmentation produced by the steps before the AdaBoost classifier, while the columns "DSC - Final" present the DSC values for the final segmentation, after the AdaBoost classifier and selection of the largest component. Cases are identified by the number present in the original files from the BRATS database.

The maximum "DSC - Close" and "DSC - Final" values obtained were 93.8% and 95.0% (case "pat466"), with an average "DSC - Close" of 59.4%

and average "DSC - Final" of 70.3%. Segmentation examples are shown in figures 2 and 3. In those figures, the left side presents the original FLAIR images, while the right side presents the final segmentation results for those cases. The blue regions represent "true positives", while the yellow regions represent "false positives" and the red regions, "false negatives". The mean time necessary to segment each image was 6.22 minutes.

4 DISCUSSION

The average final DSC value of 70.3% obtained falls into the expected interval of performance values for algorithms in this type of application. In comparison, the state-of-art algorithms tested during the BRATS challenge using a slightly bigger dataset achieved mean DSC between 19% and 81% for "whole tumor" segmentation of low-grade gliomas, with a theoretical upper limit of individual algorithmic segmentation of 86% and one fused algorithm, created by combining four different state-of-art methods, achieving mean DSC of 68% in the same task (Menze et al., 2015).

For the state-of-art algorithms of the BRATS challenge, average computation times per case ranged from few minutes to more than an hour, varying significantly between algorithms. While a direct com-

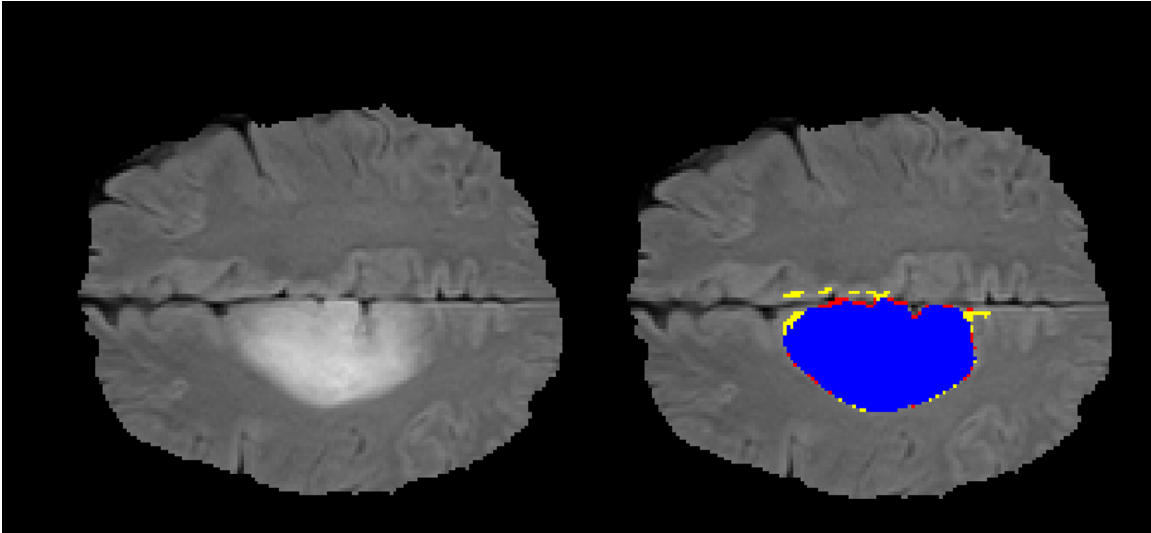


Figure 2: Segmentation example, case “pat466”, DSC 95%.

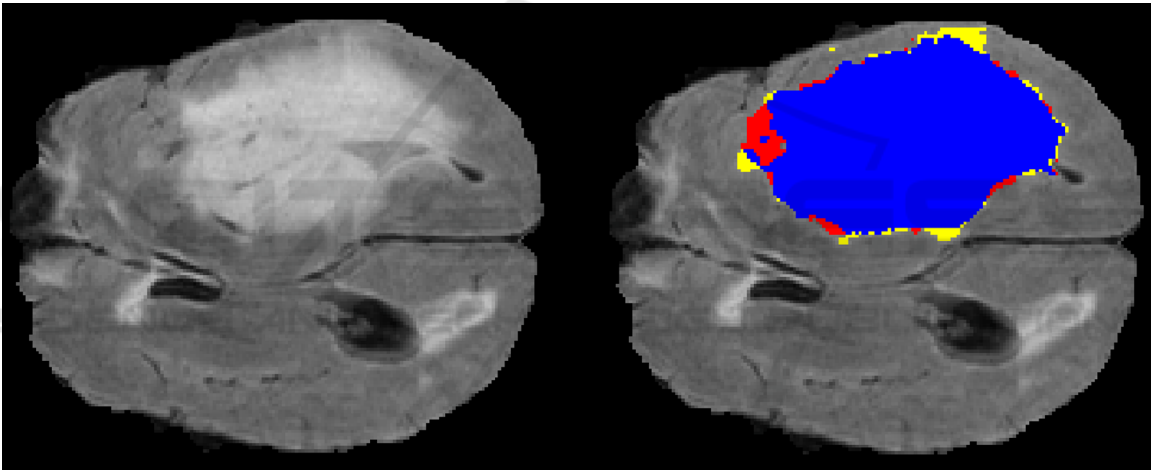


Figure 3: Segmentation example, case “pat254”, DSC 93%.

parison with our method is not possible, since the hardware used was different, it is worth noting the relatively small computational time of our method. Reduced run time is a valuable feature that should be pursued, but without forgetting to take into account the trade-off between computation time and segmentation quality, which is an important part of the process of designing a segmentation algorithm for CAD systems (Menze et al., 2015).

Our implementation of the genetic algorithm clustering method presents some differences from the original. Through our tests, it was observed that using a population of 10 individuals and two to five groups is sufficient to separate the pixels for the initial segmentation. Also, selecting between the minimum values of the clusters with higher mean intensities as threshold produces higher DSC values, as it allows

for more flexibility in the thresholding operation. In comparison, (Kole and Halder, 2012) used 30 individuals, selected tumor pixels from the cluster with highest mean intensity, and empirically selected the maximum number of groups for each image.

The percentage used for comparison between the tumor and brain area was found empirically. This comparison, together with the selection of the largest connected component, is useful in eliminating “false positives” that are created by tissues in the brain that present themselves in the original FLAIR image as high intensity regions, even though they are healthy.

In most cases, the AdaBoost classifier increased the quality of the segmentation, improving, on average, the DSC in about 10%. The choice of features – intensity and position in the slice – takes advantage of the fact that, while different tumor structures

may present themselves with different intensity values, they are formed by contiguous regions of tissue, and their position in consecutive slices do not deviate much. However, the internal boundaries between tumor tissues and the external boundaries between tumor and healthy tissue, where tissue intensity may change abruptly, might be a source of error. Including adequate texture features, for example, may improve overall performance.

One limitation to our study is the relatively small number of images available to evaluate the technique, although it is common practice in the literature to use small private datasets to evaluate segmentation methods (Menze et al., 2015). Using more images would provide a clearer picture of the proposed algorithm's performance and areas for improvement. Another limitation is that the proposed technique heavily relies on pixel intensity information, which is subject to inter and intra slice variations caused by inhomogeneity in the magnetic resonance imaging field (Emblem et al., 2009).

5 CONCLUSION

In conclusion, the method proposed in this paper combines a genetic algorithm-based clustering method with filters, morphological operation and an AdaBoost classifier to automatically isolate the tumor in magnetic resonance images. For the genetic algorithm, improvements were achieved in comparison to the original version: use of smaller population and a fixed, small number of groups to perform the clustering, which allows for less computational effort. Another difference is the strategy that makes use of the groups with highest and 2nd-highest mean intensities, allowing for adaptive restriction in the initial segmentation. Additionally, the AdaBoost classifier improved segmentation results by taking advantage of both spatial and intensity information.

Future work may focus on improving the accuracy of this technique, by adapting it to evaluate and include information from other magnetic resonance modalities, such as T1-weighted. Also, the algorithm can be further developed by adding methods to analyze texture features and better tuning of its numerical parameters, such as the percentage of area for comparison between brain and tumor tissue and the number of rounds used to train the AdaBoost classifier. Another option is to combine it with other machine-learning techniques, such as support vector machines, and create a segmentation based on the consensus of two or more classification methods.

ACKNOWLEDGEMENTS

The authors would like to thank the support by grants from São Paulo Research Foundation (FAPESP), Brazilian Federal Agency for Support and Evaluation of Graduate Education (Capes) and National Council for Scientific and Technological Development (CNPq).

REFERENCES

- Alpaydin, E. (2014). *Introduction to machine learning*. MIT press.
- Emblem, K. E., Nedregaard, B., Hald, J. K., Nome, T., Due-Tønnessen, P., and Bjørnerud, A. (2009). Automatic glioma characterization from dynamic susceptibility contrast imaging: Brain tumor segmentation using knowledge-based fuzzy clustering. *Journal of Magnetic Resonance Imaging*, 30(1):1–10.
- Freund, Y. and Schapire, R. E. (1995). A decision-theoretic generalization of on-line learning and an application to boosting. In *European conference on computational learning theory*, pages 23–37. Springer.
- Gibbs, P., Buckley, D. L., Blackband, S. J., and Horsman, A. (1996). Tumour volume determination from mr images by morphological segmentation. *Physics in medicine and biology*, 41(11):2437–2446.
- Gordillo, N., Montseny, E., and Sobrevilla, P. (2013). State of the art survey on mri brain tumor segmentation. *Magnetic resonance imaging*, 31(8):1426–1438.
- Johns Hopkins Medicine Health Library (2017). Gliomas. [online] Hopkinsmedicine.org. Available at: <https://goo.gl/8Ggjp8>. [Accessed 15 Jul. 2017].
- Kole, D. K. and Halder, A. (2012). Automatic brain tumor detection and isolation of tumor cells from mri images. *International Journal of Computer Applications*, 39(16):26–30.
- Menze, B. H., Jakab, A., Bauer, S., Kalpathy-Cramer, J., Farahani, K., Kirby, J., Burren, Y., Porz, N., Slotboom, J., Wiest, R., et al. (2015). The multimodal brain tumor image segmentation benchmark (brats). *IEEE transactions on medical imaging*, 34(10):1993–2024.
- Schapire, R. E. (1999). A brief introduction to boosting. In *Ijcai*, volume 99, pages 1401–1406.
- Sonka, M., Hlavac, V., and Boyle, R. (2014). *Image processing, analysis, and machine vision*. Cengage Learning.